




Cerium dioxide and composites for the removal of toxic metal ions

Sharon Olivera¹ · K. Chaitra² · Krishna Venkatesh² · Handanahally Basavarajaiah Muralidhara² · Inamuddin^{3,4,5}  · Abdullah M. Asiri^{3,4} · Mohd Imran Ahamed⁶

Received: 23 April 2018 / Accepted: 30 April 2018 / Published online: 8 May 2018
© Springer International Publishing AG, part of Springer Nature 2018

Abstract

The presence of contaminants in potable water is a cause of worldwide concern. In particular, the presence of metals such as arsenic, lead, cadmium, mercury, chromium can affect human health. There is thus a need for advanced techniques of water decontamination. Adsorbents based on cerium dioxide (CeO_2), also named ‘ceria,’ have been used to remove contaminants such as arsenic, fluoride, lead and cadmium. Ceria and composites display high surface area, controlled porosity and morphology, and abundance of functional groups. They have already found usage in many applications including optical, semiconductor and catalysis. Exploiting their attractive features for water treatment would unravel their potential. We review the potential of ceria and its composites for the removal of toxic metal ions from aqueous medium. The article discusses toxic contaminants in water and their impact on human health; the synthesis and adsorptive behavior of ceria-based materials including the role of morphology and surface area on the adsorption capacity, best fit adsorption isotherms, kinetic models, possible mechanisms, regeneration of adsorbents; and future perspectives of using metal oxides such as ceria. The focus of the report is the generation of cost-effective oxides of rare-earth metal, cerium, in their standalone and composite forms for contaminant removal.

Keywords Ceria · Metal ion · Composite · CeO_2 · Arsenic · Water purification

Introduction

The presence of toxic metal ions, especially heavy metal ions in water even in trace concentrations, is regarded as harmful for human health (Martin and Griswold 2009). Various regulatory organizations such as World Health Organization, Environmental Protection Agency have laid down standards for permissible levels of metal-based contaminants in water particularly potable water (Taylor 1959). As water pollution coupled with looming challenges of water scarcity deteriorates the quality of life, there have been attempts to purify water as it seems to be a viable approach. Many strategies like oxidation, floatation, reverse osmosis, adsorption, nanofiltration and biosorption have been employed for remediation contaminants mainly heavy metal ions. These technologies have trade-offs while treating water and adsorption among them is considered a practical approach owing to its simplicity of operation, cost-effective nature and efficient capture of metal ions even at low concentration (Ali 2012). A huge number of adsorbents find place in the literature. A few classes of materials used to exploit their surface phenomena are bio-based adsorbents (Bhatnagar and Sillanpää

✉ Handanahally Basavarajaiah Muralidhara
hb.murali@gmail.com

✉ Inamuddin
inamuddin@rediffmail.com

¹ Jain University, Jakkasandra Post, Kanakapura Taluk, Ramanagara District, Bangalore, Karnataka 562 112, India

² Centre for Incubation, Innovation, Research and Consultancy (CIIRC), Jyothy Institute of Technology, Thataguni, Off Kanakapura Road, Bangalore, Karnataka 560 082, India

³ Chemistry Department, Faculty of Science, King Abdulaziz University, Jeddah 21589, Saudi Arabia

⁴ Centre of Excellence for Advanced Materials Research (CEAMR), King Abdulaziz University, Jeddah 21589, Saudi Arabia

⁵ Advanced Functional Materials Laboratory, Department of Applied Chemistry, Faculty of Engineering and Technology, Aligarh Muslim University, Aligarh 202 002, India

⁶ Department of Chemistry, Faculty of Science, Aligarh Muslim University, Aligarh, Uttar Pradesh 202002, India

2010), metal oxides (Hua et al. 2012), polymers (Ge et al. 2012), graphene composites (Zhao et al. 2011), carbon nanotube composites (Chen et al. 2009), clays (Kasgoz et al. 2008) and metal organic frameworks (Khan et al. 2013).

Metal oxides as adsorbents offer wide scope for heavy metal removal. A number of metal oxides and their composites have been proven useful. Some of the metal oxides and composites investigated in the literature are zinc oxide (Kumar et al. 2013), titanium oxide (Lee and Yang 2012), iron oxide (Liu et al. 2008), layered double hydroxide–carbon nanosphere (Gong et al. 2011), iron oxide–aluminum oxide (Mahapatra et al. 2013), silica–alumina (Ismail et al. 2008), etc. Ceria which is an oxide form of rare-earth metal cerium has attracted special attention because of its high surface area values, morphological uniqueness, the possibility of occurring in different size and shape and the exposed crystal phases (Carrettin et al. 2004). However, the small size of ceria alone may become a drawback while using over filter papers as they can pass through them. The formation of composites may render useful properties to the material (Sakthivel et al. 2017).

In this article, the potential role of ceria and its composites with mainly other metal oxides or carbon-based materials for the removal of hazardous metal ions from water is reviewed. From the survey of the recent literature, it was found that hydrous ceria, ceria nanoparticles, ceria in various morphologies such as three-dimensional flower-type, hollow microspheres as well as nanospheres, nanorods, nanocubes and their combinations with graphene oxide, carbon nanotubes, silica, iron oxide, zirconia, tin oxide, manganese oxide and electrospun chitosan have been investigated in details for water purification. The target metal contaminants are arsenic, chromium, lead, mercury, cadmium, copper, nickel, vanadium, etc. Arsenic has been researched extensively compared to other metal ion contaminants. A brief of toxic effects of these contaminants on humans is provided. The core of the article deals with the synthesis strategies of cerium-based oxides as well as composites and adsorptive removal of metal ions and highlights mainly their adsorption capacity, mechanism of adsorption, isotherm model fit and kinetic model fit and regeneration of adsorbent materials for further use. Overall, a comprehensive outline of adsorption performance of ceria and its composites is provided.

Contaminants in water

Arsenic

Arsenic contamination in water takes place via several factors, some of which are arsenic leaching because of geological weathering of rocks, mining, release of industrial contaminants in the form of pesticides, dyes and paints, and processing of

minerals. It can have mutagenic, chronic neurotoxic and carcinogenic effects on humans over long-time exposure (Raichur and Panvekar 2002; Hokkanen et al. 2015). The Environmental Protection Agency of United States has recommended permissible limit for arsenic in potable water to be less than 0.01 mg/L (Yamamura et al. 2003).

Chromium

Chromium compounds find extensive use in metallurgical, chemical and refractory applications. Hexavalent chromium (Cr^{6+}) is identified as a potential mutagen and carcinogen. However, trivalent chrome is not toxic (Albadarin et al. 2013). Council of the European Union has put restrictions on the occurrence of Cr^{6+} to be lower than 0.05 mg/L (Recillas et al. 2010).

Fluoride

The permissible level of fluoride in drinking water needs to be in the range 0.7–1.5 mg/L. When present in excess, fluoride (F^-) may cause dental fluorosis and skeletal fluorosis. Fluoride is commonly observed in water bodies of developing nations, and its arrest at the source is immediately needed. Environmental Protection Agency of United States has set a standard of 4 mg/L of fluoride in industrial discharge (Naim et al. 2012; Mohapatra et al. 2012).

Lead

Toxic lead (Pb^{2+}) is generally released in water stream by processes such as dyeing, petroleum industry, tannery, smelting, galvanization, mineral processing. The World Health Organization limit for lead in potable water is 0.01 mg/L. The consumption of lead above safe levels can lead to attack on central nervous system and reproduction system. It can also adversely affect liver and kidneys (Huang and Pan 2016).

Cadmium

The World Health Organization limit for cadmium (Cd^{2+}) presence in drinking water is 0.003 mg/L. The associated risks of exposure to cadmium include itai–itai disease and renal complications. It is produced mainly by battery industries and electroplating industries (Järup et al. 1998).

Common methods of synthesis of ceria

Ceria has been generally synthesized by methods such as precipitation, solvothermal/hydrothermal, hexamethylenetetramine-based route, Kirkendall approach and

tetrabutylammonium bromide surfactant-based method. With the help of these methods, ceria was obtained in different morphologies such as three-dimensional flower hierarchical structure, hollow nanospheres, hollow nanostructures, nanocubes, nanorods etc.

Lin and Chowdhury (2010) reported exhaustively on the prominent methods of Ceria synthesis, especially in nanostructures (Lin and Chowdhury 2010). They categorized preparation processes mainly as surfactant-based and non-surfactant-based methods. The surfactant-based approach employed hard or soft templates to result in formation of nanorods (Sun et al. 2005), nanocubes (Pan et al. 2008a), nanotubes (Fuentes et al. 2008), nanowires/nanofibers (Qizheng et al. 2008) and nanobeads (Zhang et al. 2009) while non-surfactant-based methods relied on Kirkendall effect or Ostwald ripening to produce nanobeads and other nanostructures (Vantomme et al. 2005). The proposed pathway of synthesis for nanostructures of ceria is presented in Fig. 1.

The synthesis of ceria nanostructures involves the following stages of preparation: preparation of starting materials, processing of starting materials before conversion to oxides,

conversion of starting materials to mixed oxide forms and post-processing of mixed oxide materials. Such approaches have been employed not only for pristine Ceria but also for doped and mixed ceria materials. To name a few associated methods: precipitation, sol–gel, thermo-decomposition, the synthesis pathways involving colloidal solutions, emulsions and microemulsions are generally used. Alternatively, when the emphasis is to prepare one-dimensional nanocerium, surfactants and polymers are employed so as to improve physical or chemical characters like surface area, sintering resistance, reactivity (Lin and Chowdhury 2010; (Pan et al. 2008b).

Potential role of cerium-based oxides and composites in contaminant remediation

Ideally, an adsorbent for heavy metal removal must have large surface area, easily accessible pore structure, stable chemical and physical structure, specific affinity for contaminants, and suitable sizes of particles required for

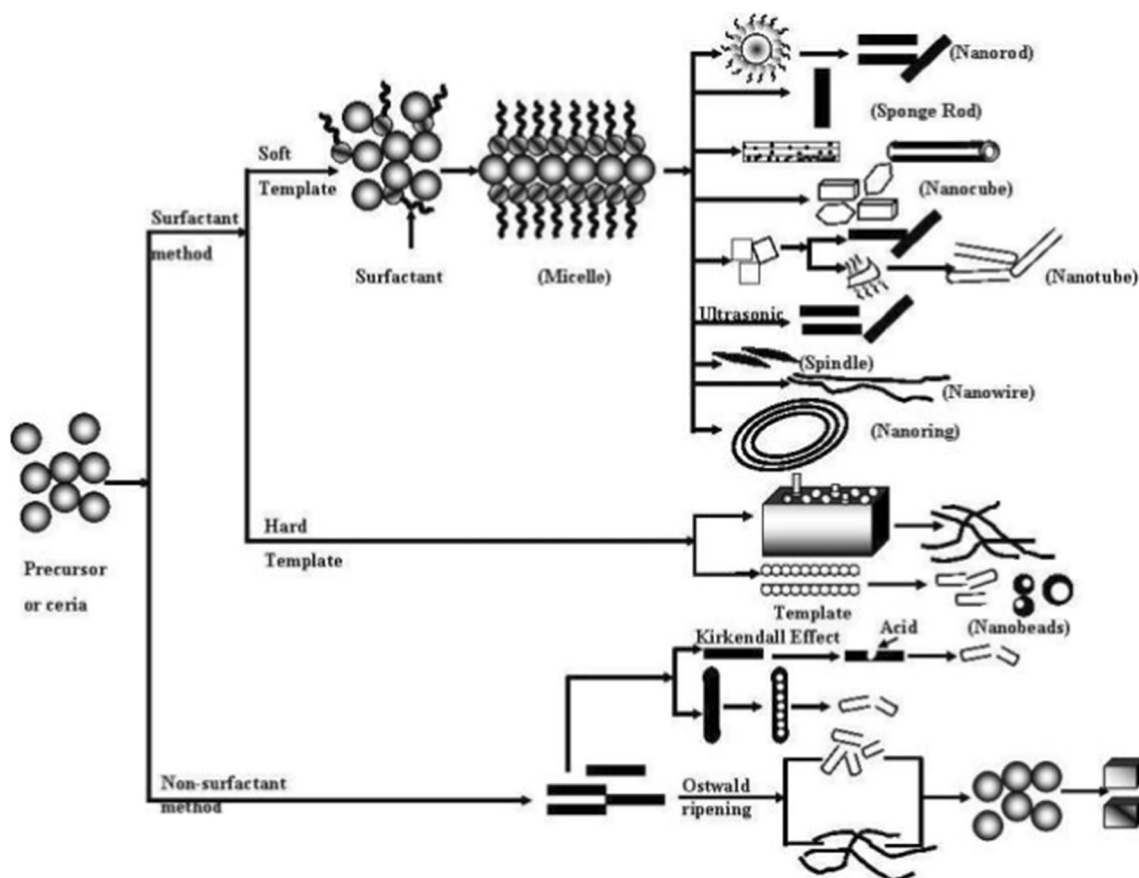


Fig. 1 Possible synthesis mechanism for formation of ceria nanostructures [reprinted with permission from (Lin and Chowdhury 2010)]. The preparation of the one-dimensional ceria nanotubes,

nanorods or nanowires was intensively studied by surfactant-assisted synthesis and surfactant-free Kirkendall coarsening, also called the Ostwald ripening method

designing bulk treatment of contaminated water (Sun et al. 2012). Cerium-based oxides and their composites have been reported to be attractive in this regard. Their performance basically originates from chemical reaction at the surface, and their reactivity is correlated with surface defects. They have been employed for sorption of contaminants such as As^{5+} , As^{3+} , Cr^{6+} , Pb^{2+} , Cd^{2+} , F^- , Hg^0 , Hg^{2+} and U^{6+} . The high surface area of ceria combined with variable morphologies offer advantages for the removal of metal ions from water. The tailoring of morphologies and particle sizes is expected to generate large surface area and innumerable adsorption site which could capture contaminants from water efficiently. Their composites with materials such as silica, graphene oxide, carbon nanotubes, manganese dioxide, iron oxide, zinc oxide, carbon cryogel and tin dioxide have been reported which have resulted in enhanced adsorption compared to their individual constituents.

Contaminant remediation by ceria and composites

Arsenic removal

In the literature, the application of ceria and its composites have been extensively explored for the removal of arsenic contaminant. In one of the pioneering works, the role of ceria anchored on carbon nanotubes was investigated for adsorption of As^{5+} from water (Peng et al. 2005). The characterization studies on as-synthesized ceria–carbon nanotubes showed homogeneous dispersion of nanoceria (particle size = 6 nm) over carbon nanotubes' surface. The composite exhibited an enhanced surface area of $189 \text{ m}^2/\text{g}$ compared to $153 \text{ m}^2/\text{g}$ of bare carbon nanotubes. The experimental results revealed that ceria–carbon nanotubes could capture up to 19.7 mg/g of As^{5+} at pH 3.1 in contrast to 8.7 mg/g at pH 10. This behavior was attributed to electrostatic interaction between ceria–carbon nanotubes and As^{5+} . It is known that As^{5+} exists as negatively charged species in water, while the charge of ceria–carbon nanotubes is dependent on solution pH. It is to be noted that when pH of solution was lower than PZC (points of zero charge, 5.5–6.4 in the present case), the adsorbent surface was positively charged, leading to feasible interaction between ceria–carbon nanotubes and As^{5+} . Electrostatic repulsion prevailed at $\text{pH} > \text{PZC}$ which resulted in decreased removal of As^{5+} . The adsorption data were fitted with Freundlich model with R^2 value of 0.964. The adsorption mechanism of As^{5+} on ceria–carbon nanotubes was explained based on chemical equilibrium of $\text{H}_2\text{AsO}_4^{2-}$ species with HAsO_4^{2-} for pH range of 3–7. Figure 2 shows proposed adsorption pathway of As^{5+} adsorption by ceria–carbon nanotubes (Peng et al. 2005).

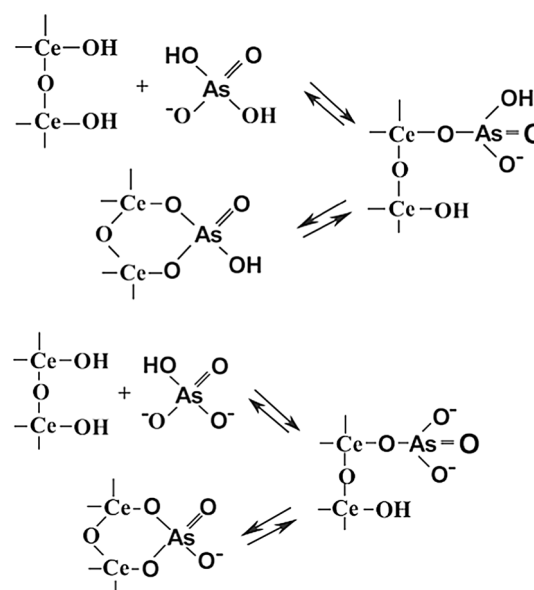


Fig. 2 Adsorption mechanism for As^{5+} adsorption on ceria–carbon nanotubes [reprinted with permission from Peng et al. (2005)]. The adsorption mechanism of As^{5+} on ceria–carbon nanotubes was explained based on chemical equilibrium of $\text{H}_2\text{AsO}_4^{2-}$ species with HAsO_4^{2-} for pH range of 3–7

Zhong et al. (2007) and Hu et al. (2008) studied ceria material that was composed of three-dimensional flower-like morphology and hierarchical structure for the removal of As^{5+} from aqueous solutions. This sorbent endowed with interconnected micro- and nanostructures combined attractive properties of huge surface area, large surface-to-volume ratio, unique size and shape as well as useful chemical functionalities desirable for heavy metal sorption. This adsorbent was particularly advantageous because the nanostructured building blocks helped retain large surface areas, overall micrometer size of material (4–6 μm) made possible easy separation and regeneration, while flowerlike morphology was useful in inhibiting agglomeration and facilitating mass transfer. When employed for As^{5+} removal at initial concentration of 13 mg/L , the as-synthesized ceria could sorb about 6.7 mg/g of heavy metal ions. Langmuir model corroborated adsorption results at different initial As^{5+} concentrations. Upon regeneration with alkali solution, ceria showed 3.3 mg/g of adsorption capacity which was higher than that of commercial ceria sorbent that removed only 0.3 mg/g of As^{5+} at initial concentration of 39 mg/L (Zhong et al. 2007; Hu et al. 2008).

Monodispersed hollow nanospheres of ceria with average size of 260 nm were fabricated by a microwave treatment procedure without the aid of any organic template or solvent. Figure 3 shows formation of hollow nanospheres which underwent Ostwald ripening pathway and involved the conversion of amorphous solid sphere into nanocrystals in the

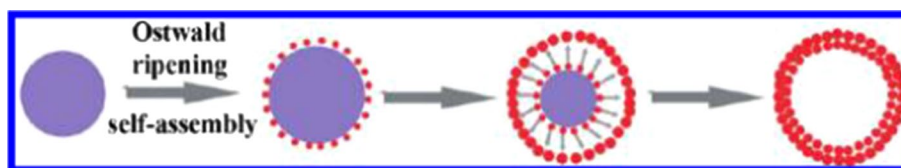


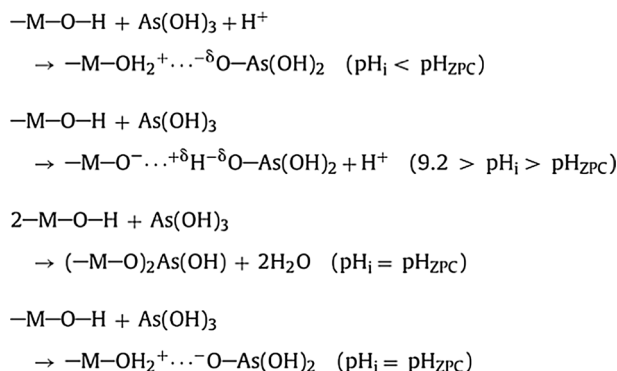
Fig. 3 Template-free synthesis of ceria hollow nanospheres involving Ostwald ripening mechanism [reprinted with permission from Cao et al. (2010)]. The hollow nanospheres undergo Ostwald ripening

intermediate stage. It was observed that 30-nm-thick shell of nanospheres comprised smaller nanoparticles. The ceria hollow nanospheres with surface area of 72 m²/g exhibited maximum Langmuir adsorption capacity of 22.4 mg/g of As⁵⁺ ions when initial concentration of 13 mg/L was maintained. The adsorbent was claimed to be easily recycled using alkali solution. The adsorption mechanism was proposed to be combination of electrostatic attraction and ion exchange (Cao et al. 2010).

Gupta et al. (2011), Feng et al. (2012), Li et al. (2012), Sun et al. (2012) and Basu and Ghosh (2013) formed mixed metal oxides of manganese and cerium as well as iron and cerium, and tested for adsorptive removal of As⁵⁺ from contaminated water. The nanocrystalline manganese dioxide–ceria adsorbent having Mn/Ce ratio of 1:1, produced by redox-assisted co-precipitation process, was proven best for As⁵⁺ capture. It had a surface area of 116.96 m²/g, average diameter of 70–90 nm and presented irregular morphology on account of aggregation. Manganese dioxide–ceria showed maximum removal percentages for pH values up to 6. This is because, when pH_{PZC} was lower than 6.5, the cationic adsorbent surface electrostatically adsorbed H₂AsO₄²⁻ and HAsO₄²⁻ quite strongly. Equilibrium of adsorption was described well with pseudo-second-order kinetic model and Freundlich equation (Gupta et al. 2011). The subsequent work on Fe(III)–Ce(IV) oxides by the same group of researchers reported the application of agglomerated nanocrystalline composite having particle size between 10 and 20 nm, surface area of 104 m²/g and pH_{PZC} of 7.13 for the removal of As⁵⁺ and As³⁺ ions from water. The adsorption capacities determined by fitting pseudo-second-order kinetic model were equal to 2.42 and 2.11 for As³⁺ and As⁵⁺, respectively. The proposed mechanism of adsorption of As⁵⁺ involved the interaction of adsorbent with H₂AsO₄²⁻ at pH 3–6, HAsO₄²⁻ at pH 8–10.5 and both species between pH range of 6–8. The mechanism of As³⁺, however, was comprised of steps shown in Scheme 1 (Basu and Ghosh 2013).

Ceria nanoparticles synthesized by precipitation method were utilized for adsorption of As⁵⁺ and As³⁺ from aqueous solution. The nanoparticles had average size of 6.6 nm and surface area of 86.85 m²/g. The adsorption performance of ceria nanoparticles with As⁵⁺ and As³⁺ ions was found to

pathway and are involved the conversion of amorphous solid sphere into nanocrystals



Scheme 1 Adsorption pathway for As³⁺ adsorption by iron oxide–ceria composite [reprinted with permission of Basu and Ghosh (2013)]. The proposed mechanism of adsorption of As⁵⁺ involved the interaction of adsorbent with H₂AsO₄²⁻ at pH 3–6, HAsO₄²⁻ at pH 8–10.5

be pH dependent and independent of ionic strength, implying chemical functionalities played key role and contribution of electrostatic interactions were insignificant. The equilibrium adsorption data were corroborated with both Langmuir and Freundlich isotherm models. Thermodynamic studies showed that adsorption process was endothermic and efficient at higher temperatures. The adsorption of As⁵⁺ was correlated with the presence of H₂AsO₄²⁻ and HAsO₄²⁻ between pH range 2–8, while As³⁺ was present as As(OH)₃ (Feng et al. 2012).

Li et al. (2012) and Sun et al. (2012) prepared hydrous ceria nanoparticles by precipitation as a part of their initial study and subsequently integrated hydrous ceria nanoparticles on silica monoliths and investigated for the removal of As⁵⁺ and As³⁺ ions. The hydrous ceria showed As³⁺ uptake capacity of 170 mg/g and As⁵⁺ uptake of 107 mg/g owing to large surface area of 198 m²/g and the presence of hydroxyl functionalities on surface. Adsorption results matched well with Redlich–Peterson isotherm model and pseudo-second-order kinetics model. Adsorption was maximum for As⁵⁺ at pH 3, whereas hydrous ceria presented high adsorption for As³⁺ at pH 7. The former species would be present as H₂AsO₄²⁻ and HAsO₄²⁻ between pH 2.2 and 11, while latter occurs as As(OH)₃ when pH is less than 9.2 and as H₂AsO₃⁻

for pH higher than 9.2. Hydrous ceria nanoparticles would carry lower density of negative charges at high pH values, and thus, it showed maximum removal of As^{5+} at acidic pH due to coulombic attraction. As for As^{3+} , charge-less $\text{As}(\text{OH})_3$ did not hinder electrostatic interaction till pH of 9.2 and caused adsorption to decrease after this pH due to coulombic repulsion between anionic surface of hydrous ceria and H_2AsO_3^- (Li et al. 2012). Upon impregnation of hydrous ceria with silica skeleton, the resultant composite possessed interlinked micro-sized macropores useful for easy movement of water and enormous mesopores of silica beneficial for ceria nanoparticle adherence. This novel composite was reported for arsenic remediation of synthetic and natural water samples. It showed faster kinetics for both contaminants, for example, it achieved As^{3+} removal percentage of 85% within 30 min for initial concentration of 106 $\mu\text{g/L}$. Pseudo-second-order model was in agreement with kinetics data. Equilibrium uptake capacities of 7 mg/g and 6.84 mg/g were obtained for As^{3+} and As^{5+} , respectively. The adsorbent was recycled with dilute hydrogen peroxide and reused (Sun et al. 2012). The same group of researchers developed paper-like trimanganese tetroxide–ceria membranes with surface area of 98 m^2/g formed by spontaneous exfoliation of their hybrid nanotube intermediates for adsorption of As^{3+} from water. The synthesis strategy steps are shown in Fig. 4.

The composite membrane performed excellently in continuous flow-through tests when As^{3+} solutions of initial concentration of 96 $\mu\text{g/L}$ were injected through it. It retained 85% of its removal capacity after 36th injection of contaminant. The membrane was successfully regenerated using sodium hydroxide and recycled (Guo et al. 2015).

Hierarchically porous zirconia–ceria nanospheres were prepared in a study to evaluate their adsorption on pentavalent and trivalent arsenic in water. The amorphous nanospheres had an external diameter of 90 nm and surface area of 29.61 m^2/g . It consisted of both mesopores and macropores which were beneficial for fast diffusion and mass transfer. The porous network of adsorbents coupled

with huge number of hydroxyl groups as active sites aided in enhanced uptake of arsenic pollutant. It was reported that zirconia–ceria could sorb up to 97% of arsenic when initial concentration of 0.376 mg/L was used. Substitution of hydroxyl by arsenic was proposed as possible mechanism for adsorption. Pseudo-second-order model was fitted better for adsorption kinetics. Maximum removal of As^{5+} and As^{3+} was observed at highly acidic and mildly basic pH conditions, respectively. This is because zirconia–ceria composite had its pH_{PZC} equal to 7.8 which meant it would carry positive charge below that pH value and would have negative charge above 7.8. The presence of anionic species of As^{5+} in acidic pH and neutral species of As^{3+} at alkaline pH favored above-mentioned adsorption pattern (Xu et al. 2013).

Hydrothermally prepared nanostructured hollow iron–cerium alkoxide was utilized for As^{5+} and As^{3+} sorption. The adsorbent had large surface area of 217.5 m^2/g and huge density of chemical functionalities. It showed higher affinity toward As^{3+} than As^{5+} . The mechanism of As^{5+} removal was proposed to include ion exchange with negatively charged hydroxyl groups on the surface, carbonate and unidentate carbonate-type species. The adsorption isotherms were in agreement with Langmuir and Freundlich models, respectively, for As^{5+} and As^{3+} indicating monolayer and multilayer adsorptions. The dominance of $\text{H}_2\text{AsO}_4^{2-}$ and HAsO_4^{2-} species in case of As^{5+} and H_3AsO_3 and in case of As^{3+} was responsible for adsorption performance. Kinetic results were matched well with pseudo-second-order kinetic model (Chen et al. 2014). A nanometer-sized ceria-deposited iron–silica was employed for in situ trapping of arsenic hydrides. Upon extraction, the sorbent was separated by magnetic means and subjected to analysis. The magnetic composite exhibited trapping efficiency of 94% for As (Dados et al. 2014a). Cerium-immobilized electrospun chitosan–polyvinyl alcohol composites were investigated for As^{3+} capture from water. Adsorption experiments revealed the matching of Langmuir isotherm to adsorption equilibrium with maximum adsorption capacity of 18.0 mg/g for

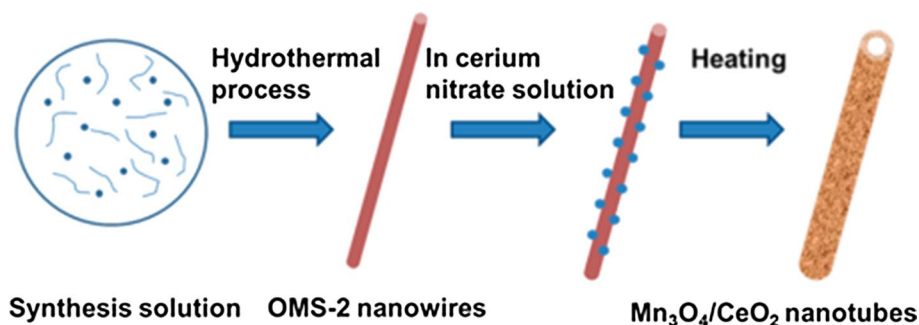


Fig. 4 Representation of synthesis of trimanganese tetroxide–ceria hybrid nanotubes prior to membrane formation. OMS-2 denotes cryptomelane-type manganese oxide template, Mn_3O_4 =manganese

tetroxide and CeO_2 =ceria [reprinted with permission from Guo et al. (2015)]. The spontaneous exfoliation of hybrid nanotube intermediates resulted in membranes useful for adsorption of As^{3+} from water

As³⁺. Kinetic data were fitted better with pseudo-second-order model. The possible mechanism of As³⁺ adsorption is provided in Fig. 5. The regeneration studies done on arsenic saturated adsorbent with dilute hydrochloric acid showed a drop up to 35% after three cycles. The reason was attributed to deformation of nanofiber in hydrochloric acid (Sharma et al. 2014).

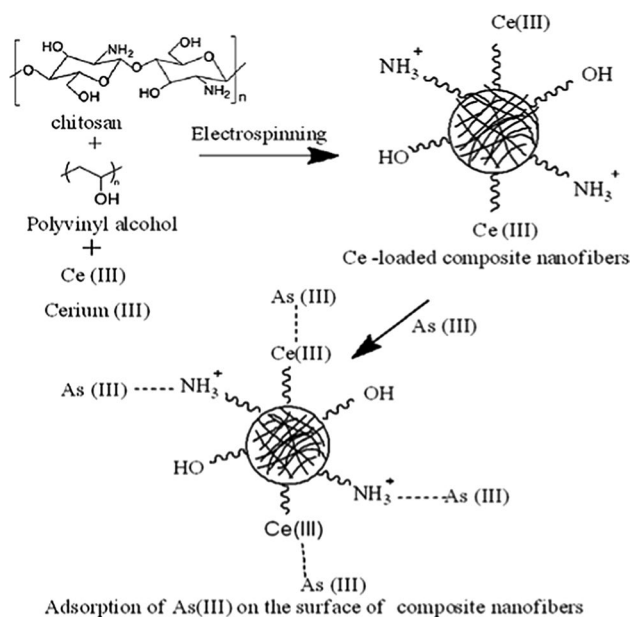


Fig. 5 Possible adsorption mechanism for As³⁺ on cerium-immobilized electrospun chitosan–polyvinyl alcohol [reprinted with permission from Sharma et al. (2014)]. When solution pH is acidic, large number of cationic surface sites are generated by protonation of amino groups on chitosan and highly electropositive Ce(III) that effectively capture As³⁺

A bionanocomposite based on zinc oxide, ceria, nanocellulose and polyaniline was fabricated for remediation of arsenic. The characterizations on as-prepared composite revealed the presence of nanosized zinc oxide and ceria in nanocellulose–polyaniline framework. Zinc oxide had average diameter of 85–124 nm, while ceria size was 1.6 nm at an average. More than 95% of arsenic contaminant was eliminated when adsorbent was employed for initial As concentration of 10 ppb. The availability of abundant hydroxyl groups of cellulose and polymeric chain was proposed to favor complexation with As ions. Further, primary and tertiary amines of polyaniline were also claimed to contribute to larger adsorption capacity. Maximum adsorption of As ions was observed at pH of 8. Adsorption isotherms were in close agreement with Freundlich and Dubinin–Radushkevich isotherm models and pseudo-second-order model described adsorption well (Nath et al. 2016). Trivalent arsenic contaminant removal was probed on carbon cryogel/ceria nanocomposite. The adsorbent possessed surface area of 614 m²/g, and the ceria was dispersed homogeneously in large pores of carbon cryogel. From solution of As³⁺ with initial concentration of 10 mg/L, 93% of contaminant was adsorbed in just 10 min. Adsorption kinetics obeyed pseudo-second-order kinetic equation. Maximum As³⁺ removal was noticed at pH values lower than 5 (Minovic-Arsic et al. 2016).

Sakthivel et al. (2017) prepared ceria–graphene oxide composite for eliminating As⁵⁺ and As³⁺ from water. The synthesis of ceria–graphene oxide is presented in Fig. 6. The composite showed a flake-like morphology having about 1 μm particle size. For initial arsenic concentrations of 0.1 mg/L, ceria–graphene oxide achieved maximum removal of 99.99% within 10 min of reaction with adsorbent doses of 0.2 and 0.4 mg/L for As³⁺ and As⁵⁺, respectively (Sakthivel et al. 2017).

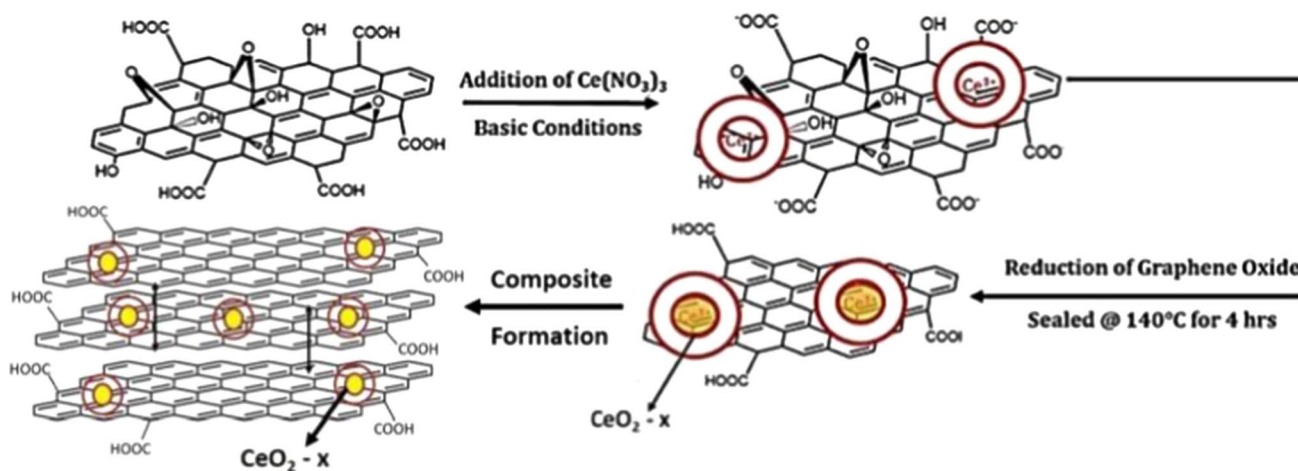


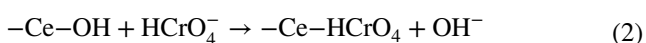
Fig. 6 One-step hydrothermal synthesis of ceria–graphene oxide composite [reprinted with permission from Sakthivel et al. (2017)]. The synthesis was carried out by mixing graphene oxide and ceria

precursors, ammonium hydroxide was added to maintain basic pH, and thermal treatment was carried out to obtain desired product

The adsorption capacities of various ceria-based adsorbents for As^{3+} and As^{5+} are provided in Table 1.

Chromium removal

Hexavalent chromium removal was investigated on ceria anchored on aligned carbon nanotubes. The major adsorption was found to occur between pH of 3.0 and 7.4. The hydroxylated ceria immobilized on aligned carbon nanotubes interacted electrostatically with CrO_4^{2-} and HCrO_4^- species prevalent at this pH range to give this result. The mechanism involved the reactions given in Eqs. 1 and 2.



The maximum adsorption capacity of 30.2 mg/g was obtained for initial Cr^{6+} concentration of 35.3 mg/L at pH of 7. Langmuir isotherms showed better agreement with equilibrium adsorption data (Di et al. 2006). The microspheres of ceria nanocrystals with three-dimensional hierarchical structure having surface area of 65 m^2/g developed by sol-gel approach were studied for Cr^{6+} ions from water. Freundlich and pseudo-second-order kinetic models were fitted better for adsorption results. The adsorbent was reported to have taken up 6.81 m^2/g of Cr^{6+} at pH equal to 8.0 (Xiao et al. 2009).

Recillas et al. (2010), Contreras et al. (2015) and Mercado-Borrayo et al. (2018) prepared

hexamethylenetetramine-stabilized ceria in nanosize and utilized for Cr^{6+} removal from aqueous phase. The equilibrium and kinetics of adsorption were effectively expressed by Freundlich and pseudo-second-order kinetic models. Ceria nanoparticles removed about 83.33 mg/g of Cr^{6+} ions from solution of 37.5 mg/L initial concentration. Electrostatic attraction between anionic Cr^{6+} and hydroxylated cationic ceria surface at neutral pH was proposed as possible mechanism of adsorption (Recillas et al. 2010).

Monodispersed hollow nanospheres of ceria with average size of 260 nm fabricated by a microwave treatment procedure exhibited adsorption capacity of 15.4 mg/g from initial Cr^{6+} concentration of 26.8 mg/L (Cao et al. 2010). Ceria nanopowder synthesized for Cr^{6+} elimination from water successfully achieved up to 90% removal within the first 30 min of adsorption process when initial Cr^{6+} concentration of 10 mg/L was used (Jena 2012). In another study, monodispersed hollow ceria nanospheres with surface area of 76.86 m^2/g and average diameter of 400 nm were loaded with 70% Cr^{6+} ions that were three times higher than commercial ceria powder (Jiangtao 2016).

Hydrous ceria prepared by precipitation method could remove 99% of Cr^{6+} ions from 1.923 mM initial metal concentration at pH of 2. The reason for high adsorption at pH 2 was claimed to be due to electrostatic interaction between negative species of Cr^{6+} occurring at that pH and cationic adsorbent surface. Adsorption efficiency lowered with the increase in pH from 3 to 10 because the pH_{PZC} or isoelectric point existed at pH of 2.7. The adsorption capacity of

Table 1 As^{3+} and As^{5+} adsorption capacities of ceria and composite materials

Adsorbent	Contaminant	Maximum adsorption capacity (mg/g)	References
3D Flowerlike ceria	As^{5+}	14.4	Zhong et al. (2007), Hu et al. (2008)
Ceria-carbon nanotubes	As^{5+}	81.9 ^a	Peng et al. (2005)
Ceria hollow nanospheres	As^{5+}	22.4	Cao et al. (2010)
Manganese dioxide-ceria	As^{5+}	18.653	Gupta et al. (2011)
Ceria nanoparticles	As^{5+}	17.08	Feng et al. (2012)
Hydrous ceria	As^{5+}	107.1	Li et al. (2012)
Hydrous ceria	As^{3+}	171.88	Li et al. (2012)
Manganese tetroxide-ceria hybrid nanotubes	As^{3+}	160.0	Guo et al. (2015)
Zirconia-ceria	As^{5+}	145.35	Xu et al. (2013)
Zirconia-ceria	As^{3+}	110.7	Xu et al. (2013)
Nanostructured hollow iron-cerium alkoxide	As^{5+}	206.6	Chen et al. (2014)
Nanostructured hollow iron-cerium alkoxide	As^{3+}	260.0	Chen et al. (2014)
Cerium-loaded electrospun chitosan-polyvinyl alcohol	As^{3+}	18.2	Sharma et al. (2014)
Ceria-graphene oxide	As^{5+}	215.0	Sakthivel et al. (2017)
Ceria-graphene oxide	As^{3+}	185.0	Sakthivel et al. (2017)
Ceria-iron oxide	As^{3+}	8.260	Ansari et al. (2017)

^a $[\text{Ca}^{2+}] = 10 \text{ mg/L}$; tested in the presence of calcium ions

Table 2 Adsorption capacities of ceria and its composites for Cr⁶⁺ adsorption

Adsorbent	Maximum adsorption capacity	References
Ceria/aligned carbon nanotubes	31.55 mg/g	Di et al. (2006)
Ceria microspheres	6.76 mg/g	Xiao et al. (2009)
Ceria nanoparticles	121.95 ^a mg/g	Recillas et al. (2010)
Ceria hollow nanospheres	15.4 mg/g	Cao et al. (2010)
Ceria nanoparticles	34.4 mg/g	Contreras et al. (2015)
Hydrous ceria	0.828 mmol/g	Albadarin et al. (2014)

^aInitial Cr⁶⁺ concentration = 80 mg/L

0.83 mmol/g was found by corroborating adsorption data with Langmuir model (Albadarin et al. 2014) (Table 2).

Fluoride removal

Zhang et al. (2011) and Zhang et al. (2013) studied the removal of fluoride ions from water by nonthermal plasma-treated ceria/Al₂O₃ composite with special consideration of kinetics and equilibrium of adsorption. Adsorption process followed Langmuir isotherm model and pseudo-second-order kinetic equation. About 45 mg/g of adsorption capacity was noted for ceria/alumina composite toward fluoride ions when 125 mg/L of initial metal ion concentration was utilized. The mechanism basically involved ion exchange between F⁻ and OH⁻ ions. Thermodynamic studies revealed spontaneity and feasibility of adsorption (Zhang et al. 2011). In the presence of competing anions, the adsorption capacity was seen to decrease in the order: Cl⁻ < NO₃⁻ < SO₄²⁻ < CO₃²⁻ < C₂O₄²⁻ < HPO₄²⁻. The divalent cations were found to give higher competition for active site of adsorbent compared to monovalent ones (Zhang et al. 2013).

Kang et al. (2017) evaluated the influence of different morphologies of ceria material for F⁻ adsorption from aqueous solution. At pH 3, ceria with nanorod structure (average size = 15–25 nm) whose (100) and (110) planes were available for adsorption of F⁻ showed higher adsorption capacity while nanocubes (average size = 25 nm) of ceria exhibited lower adsorption because its (110) plane was only exposed for reaction. The adsorption mechanism was claimed to involve Ce³⁺–O defects, ion exchange, surface adsorption and pore filling. Langmuir and pseudo-second-order models with R² values higher than 0.99 showed better fit for adsorption data (Kang et al. 2017).

Fluoride removal by porous ceria/silica was tested at concentration as high as 400 mg/L in one of the recent studies. The analyses showed that adsorption was monolayer type and mainly chemical sorption as derived by matching

Langmuir and pseudo-second-order models of sorption. Adsorption capacity for F⁻ was equal to 2.44 mmol/g at 25 °C. The desorption studies using dilute NaOH indicated regeneration capability of composite with only 5% decrease (Lin et al. 2017) (Table 3).

Lead removal

Mercapto-modified electrospun ceria was investigated for Pb²⁺ capture from water. Polyvinyl pyrrolidone/cerium oxide/3-mercaptopropyltrimethoxysilane was employed as modification agent in the presence of surfactant P123. The adsorbent with surface area of 163.6 m²/g exhibited Langmuir adsorption capacity of 0.439 mmol/g for lead. A pH of 6 was found to be optimum for adsorption of Pb²⁺. As pH_{PZC} = 4.8, at pH values lower than it, coulombic repulsion prevailed. At pH > 6, precipitation of Pb²⁺ as lead hydroxide hindered the possibility of experiment. The double exponential model showed high correlation for adsorption kinetics (Yari et al. 2015). Ceria nanoparticles were examined for Pb²⁺ removal by Contreras et al. (2015), Mercado-Borrayo et al. (2018). Single or multilingual type of systems and pH of solution did not alter Pb²⁺ adsorption capacity. Adsorption data were successfully corroborated with polynomial functions (Contreras et al. 2015). About 34% of Pb²⁺ ions were removed efficiently by ceria nanoparticles. These nanoparticles possessed surface area of 65 m²/g (Mercado-Borrayo et al. 2018).

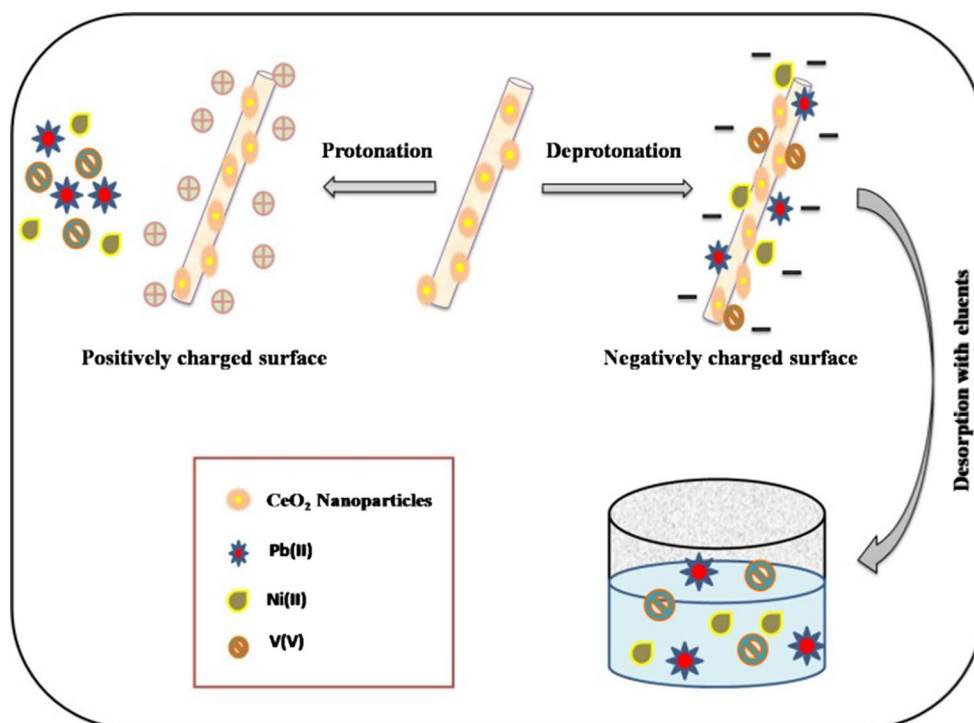
Nanofibers of ceria/CuFe₂O₄ having ceria outer shell and CuFe₂O₄ core were synthesized and studied for Pb²⁺ capture. The synthesis scheme is shown in Fig. 7. The average diameter of ceria/CuFe₂O₄ was 100 nm, and Brunauer–Emmet–Teller (BET) surface area was 190.2 m²/g. The adsorption capacity of CuFe₂O₄ was reported to be equal to 972.4 mg/g which was highest reported for ceria-based nanocomposites. Adsorption data were best fitted with Langmuir–Freundlich and Fractal-like pseudo-second-order kinetic models. The adsorbent could

Table 3 Adsorption capacities of ceria and its composites for F⁻ adsorption

Adsorbent	Maximum adsorption capacity	References
Ceria alumina	46.59 mg/g ^a	Zhang et al. (2011)
Ceria/alumina	37.0 mg/g ^{a,b}	Zhang et al. (2013)
Octahedral ceria	7.0 mg/g ^a	Kang et al. (2017)
Ceria nanocubes	28.3 mg/g ^a	Kang et al. (2017)
Ceria nanorods	71.5 mg/g ^a	Kang et al. (2017)
Ceria/silica	2.441 mmol/g	Lin et al. (2017)

Initial F⁻ concentration ^a125 mg/L; ^b120 mg/L

Fig. 7 Schematic representation of **a** synthesis of the ceria/CuFe₂O₄ composite and **b** the adsorption mechanism of metal ions [modified after Talebzadeh et al. (2016)]. The synthesis involved chemical precipitation in which CuFe₂O₄ and ceria precursor were sonicated first followed by addition of sodium hydroxide as precipitating agent



remove more than 99% of Pb²⁺ from tap water, river water and petrochemical wastewater (Talebzadeh et al. 2016).

A composite based on ceria, tin dioxide and reduced graphene oxide was studied for Pb²⁺ removal. The composite showed non-uniform distribution of ceria and tin dioxide on layered surface of reduced graphene oxide. Average diameter of particles was equal to 7–8 nm. Experiments showed that about 74% of Pb²⁺ was eliminated by ceria–tin dioxide–reduced graphene oxide in the presence of sodium chloride. Removal efficiency reached 81% at pH of 7. The interference of precipitation of Pb²⁺ as lead hydroxide was expected after pH of 7 (Priyadharsan et al. 2017) (Table 4).

Uranyl ions removal

Ceria nanocrystals with surface area of 41 m²/g were produced and checked for remediation of U⁶⁺ ions from water (Kuncham et al. 2017). The nanocrystals obeyed Langmuir adsorption and showed maximum loading of 27 mg/g of U⁶⁺ ions. Pore filling and coulombic interactions were

proposed to be responsible for adsorption mechanism. As pH_{PZC} of ceria nanocrystals was between 5.8 and 7.9, the optimum pH value was found to be 5. At lower pH values, U⁶⁺ ions were present as, and adsorbent surface was positive causing higher adsorption of U⁶⁺ ions. At pH higher than 5, U⁶⁺ ions had a tendency to remain as UO₂(CO)₂²⁻ and UO₂(CO)₃⁴⁻ causing electrostatic repulsion between anionic surface and these species. Hence, adsorption of U⁶⁺ was again decreased. After leaching experiments with 5 wt% ammonium bicarbonate, ceria adsorbent was regenerated with minimum capacity loss (Kuncham et al. 2017). Another study on removal of U⁶⁺ ions from aqueous medium included the development of ceria–titania–iron oxide composite. This composite had average particle diameter of 3.22–14.04 and surface area of 35.2 m²/g. A pH of 6 was found to be optimum for adsorption. The maximum U⁶⁺ adsorption capacity determined from Langmuir isotherm was 439.88 mg/g. Pseudo-second-order model described well the adsorption kinetics. On regeneration with 0.1 M hydrochloric acid, adsorption

Table 4 Adsorption capacities of ceria and its composites for Pb²⁺ adsorption

Adsorbent	Maximum adsorption capacity	References
Polyvinyl pyrrolidone/cerium oxide/3-mercaptopropyltrimethoxysilane	90.9	Yari et al. (2015)
Ceria	128.1	Contreras et al. (2015)
Ceria/CuFe ₂ O ₄	972.4 mg/g	Talebzadeh et al. (2016)

capacity decreased from 439.88 to 416.41 mg/g (El-sherif et al. 2017).

Mercury removal

A nanoceria-impregnated silica–iron oxide material was used for the removal of Hg^{2+} from aqueous medium. The synthesis route involved co-precipitation and sol–gel method of silica–iron oxide followed by deposition of ceria by precipitation. The adsorbent could sorb up to 50% of mercury from water in time duration of 120 min at a pH of 8. The metal-saturated adsorbent was separated easily by use of magnet (Dados et al. 2014b). A composite of ceria–zirconia–titania removed Hg^0 by catalytic oxidation method (Li et al. 2016). The schematic representation of catalytic oxidation of contaminant is shown in Fig. 8.

In another study, silica-supported ceria nanomaterials prepared by precipitation were utilized for adsorption of Hg^{2+} . Characterization studies showed silica was core, while ceria was present as the shell and both ceria and silica were spherical. Freundlich adsorption isotherm matched equilibrium adsorption data well with adsorption capacity of 153.8 $\mu\text{g/g}$ (Vaizoğullar et al. 2016).

Cadmium removal

Ceria nanoparticles were examined for Cd^{2+} removal by Contreras et al. (2015), Mercado-Borrayo et al. (2018). Single or multilingual type of systems did not alter Cd^{2+} adsorption capacity. Adsorption data were successfully corroborated with polynomial functions. The adsorption capacity of 93.4 mg/g for Cd^{2+} was determined. About 64% of Pb^{2+} ions were removed efficiently by ceria nanoparticles. These nanoparticles possessed surface area of 65 m^2/g . Ceria–tin dioxide–reduced graphene oxide composite adsorbed 78% of Cd^{2+} in the presence of sodium chloride. pH 7 was found to be optimum for adsorption (Priyadharsan et al. 2017). Another study

by Contreras et al. (2012) had reported 49.1 mg/g adsorption capacity of ceria nanoparticles. Freundlich isotherm model and pseudo-second-order model were found to fit the adsorption data (Contreras et al. 2012).

Miscellaneous contaminant removal

Some of the ceria-based composites were utilized for sorption of platinum, nickel, vanadium, silver, phosphate and copper from water (Talebzadeh et al. 2016; Liu et al. 2017; Yari et al. 2015; Farmer 2010; Bruix et al. 2010). Nanofibers of ceria/ CuFe_2O_4 having ceria outer shell and CuFe_2O_4 core adsorbed 686.1 mg/g and 798.6 mg/g of Ni^{2+} and V^{5+} , respectively. Fractal-like pseudo-second-order model and Langmuir–Freundlich models fitted the adsorption data well (Talebzadeh et al. 2016). The ceria functionalized iron oxide–silica nanomaterial with surface area of 179.7 m^2/g and mean particle size of 8.63 nm adsorbed phosphate ions of about 26.45 mg/g. Separation and reuse of adsorbent were successfully tested for four adsorption–desorption cycles (Liu et al. 2017). Mercapto-modified electrospun ceria showed maximum adsorption capacity of 263.4 mg/g for Cu^{2+} ions. A pH of 6 was found to be optimum for adsorption of Cd^{2+} . As $\text{pH}_{\text{PZC}} = 4.8$, at pH values lower than it, coulombic repulsion prevailed. At $\text{pH} > 6$, precipitation of Cd^{2+} as $\text{Cd}(\text{OH})_2$ hindered the possibility of experiment. The double exponential model showed high correlation for adsorption kinetics (Yari et al. 2015).

Future prospects of ceria and composites for water remediation

Nanosized ceria materials are regarded as industrially important due to their attractive properties (Feng et al. 2012). However, formation of composites is crucial as nanoparticles in their pristine form may be leached into environment causing harmful effects. It has been observed that metal oxides in nanosize are prone to agglomeration resulting drop in adsorption performance. Also, better means of separation of contaminant-saturated sorbents have to be developed. Even though forming composites of metal oxide with other substrates has been offered as a solution to pressure drop in flow-through systems, this research is at infant stage. The toxicity effects of ceria and composites need to be investigated to prevent possible future challenges with regard to humans and environment.

Conclusion

Removal of toxic contaminants from water is one of the urgent measures to curb the water pollution problem. In this review, ceria and its composites used for contaminant

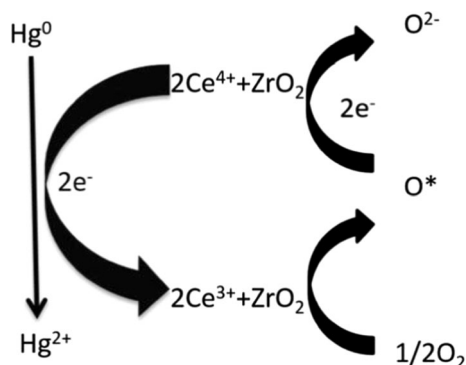


Fig. 8 Scheme of mercury removal by ceria–zirconia–titania through catalytic oxidation. ZrO_2 = zirconia [reprinted with permission from Li et al. (2016)]

remediation in the recent years have been reviewed. The adsorption of contaminants to large extents by cost-effective and efficient ceria-based adsorbents offers better alternatives for existing adsorbents. The large surface area combined with ability to form ceria and composites in variable morphological properties makes them competent adsorbents for treating toxic contaminants water. Tailoring of properties to use them for multi-purpose water treatment applications could be a key area of the research that can be explored in the future.

Acknowledgements Authors thank the Centre for Incubation, Innovation, Research and Consultancy, Jyothy Institute of Technology and Sri Sringeri Sharadha Peetam for supporting this study. Dr. Inamuddin is thankful to the King Abdulaziz University, Jeddah, Saudi Arabia, to carry out this study.

Compliance with ethical standards

Conflict of interest The authors declare that they have no conflict of interest.

References

- Albadarin AB, Mangwandi C, Walker GM et al (2013) Influence of solution chemistry on Cr(VI) reduction and complexation onto date-pits/tea-waste biomaterials. *J Environ Manage* 114:190–201. <https://doi.org/10.1016/j.jenvman.2012.09.017>
- Albadarin AB, Yang Z, Mangwandi C et al (2014) Experimental design and batch experiments for optimization of Cr(VI) removal from aqueous solutions by hydrous cerium oxide nanoparticles. *Chem Eng Res Des* 92:1354–1362. <https://doi.org/10.1016/j.cherd.2013.10.015>
- Ali I (2012) New generation adsorbents for water treatment. *Chem Rev* 112:5073–5091. <https://doi.org/10.1021/cr300133d>
- Ansari R, Hasanazadeh M, Ostovar F (2017) Arsenic removal from water samples using CeO₂/Fe₂O₃ nanocomposite. *Int J Nanosci Nanotechnol* 13:335–345
- Basu T, Ghosh UC (2013) Nano-structured iron(III)–cerium(IV) mixed oxide: synthesis, characterization and arsenic sorption kinetics in the presence of co-existing ions aiming to apply for high arsenic groundwater treatment. *Appl Surf Sci* 283:471–481. <https://doi.org/10.1016/j.apsusc.2013.06.132>
- Bhatnagar A, Sillanpää M (2010) Utilization of agro-industrial and municipal waste materials as potential adsorbents for water treatment—a review. *Chem Eng J* 157:277–296. <https://doi.org/10.1016/j.cej.2010.01.007>
- Bruix A, Neyman KM, Illas F (2010) Adsorption, oxidation state, and diffusion of Pt atoms on the CeO₂(111) surface. *J Phys Chem C* 114:14202–14207. <https://doi.org/10.1021/jp104490k>
- Cao CY, Cui ZM, Chen CQ et al (2010) Ceria hollow nanospheres produced by a template-free microwave-assisted hydrothermal method for heavy metal ion removal and catalysis. *J Phys Chem C* 114:9865–9870. <https://doi.org/10.1021/jp101553x>
- Carrettin S, Concepción P, Corma A et al (2004) Nanocrystalline CeO₂ increases the activity of Au for CO oxidation by two orders of magnitude. *Angew Chem Int Ed* 116:2592–2594. <https://doi.org/10.1002/anie.200353570>
- Chen C, Hu J, Shao D et al (2009) Adsorption behavior of multiwall carbon nanotube/iron oxide magnetic composites for Ni(II) and Sr(II). *J Hazard Mater* 164:923–928. <https://doi.org/10.1016/j.jhazmat.2008.08.089>
- Chen B, Zhu Z, Liu S et al (2014) Facile hydrothermal synthesis of nanostructured hollow iron–cerium alkoxides and their superior arsenic adsorption performance. *ACS Appl Mater Interfaces* 6:14016–14025
- Contreras AR, Garcia A et al (2012) Potential use of CeO₂, TiO₂ and Fe₃O₄ nanoparticles for the removal of cadmium from water. *Desalin Water Treat* 1–3:296–300
- Contreras AR, Casals E, Puentes V et al (2015) Use of cerium oxide (CeO₂) nanoparticles for the adsorption of dissolved cadmium(II), lead(II) and chromium(VI) at two different pHs in single and multi-component systems. *Glob NEST J* 17:536–543
- Dados A, Kartsiouli E, Chatzimitakos T et al (2014a) In situ trapping of As, Sb and Se hydrides on nanometer-sized ceria-coated iron oxide–silica and slurry suspension introduction to ICP-OES. *Talanta* 130:142–147. <https://doi.org/10.1016/j.talanta.2014.06.046>
- Dados A, Pappazou E, Eleftheriou P et al (2014b) Nanometer-sized ceria-coated silica–iron oxide for the reagentless microextraction/preconcentration of heavy metals in environmental and biological samples followed by slurry introduction to ICP-OES. *Talanta* 121:127–135. <https://doi.org/10.1016/j.talanta.2013.12.045>
- Di ZC, Ding J, Peng XJ et al (2006) Chromium adsorption by aligned carbon nanotubes supported ceria nanoparticles. *Chemosphere* 62:861–865. <https://doi.org/10.1016/j.chemosphere.2004.06.044>
- El-sherif RM, Lasheen TA, Jebri EA (2017) Fabrication and characterization of CeO₂–TiO₂–Fe₂O₃ magnetic nanoparticles for rapid removal of uranium ions from industrial waste solutions. *J Mol Liq* 241:260–269. <https://doi.org/10.1016/j.molliq.2017.05.119>
- Farmer J (2010) Ag adsorption on reduced CeO₂(111) thin films. *J Phys* 2:17166–17172. <https://doi.org/10.1021/jp104593y>
- Feng Q, Zhang Z, Ma Y et al (2012) Adsorption and desorption characteristics of arsenic onto ceria nanoparticles. *Nanoscale Res Lett* 7:1–8. <https://doi.org/10.1186/1556-276X-7-84>
- Fuentes RO, Acuña LM, Zimicz MG et al (2008) Formation and structural properties of Ce–Zr mixed oxide nanotubes. *Chem Mater* 20:7356–7363. <https://doi.org/10.1021/cm801680c>
- Ge F, Li MM, Ye H, Zhao BX (2012) Effective removal of heavy metal ions Cd²⁺, Zn²⁺, Pb²⁺, Cu²⁺ from aqueous solution by polymer-modified magnetic nanoparticles. *J Hazard Mater* 211–212:366–372. <https://doi.org/10.1016/j.jhazmat.2011.12.013>
- Gong J, Liu T, Wang X et al (2011) Efficient removal of heavy metal ions from aqueous systems with the assembly of anisotropic layered double hydroxide nanocrystals@carbon nanosphere. *Environ Sci Technol* 45:6181–6187. <https://doi.org/10.1021/es200668q>
- Guo S, Sun W, Yang W et al (2015) Synthesis of Mn₃O₄/CeO₂ hybrid nanotubes and their spontaneous formation of a paper-like, free-standing membrane for the removal of arsenite from water. *ACS Appl Mater Interfaces* 7:26291–26300. <https://doi.org/10.1021/acsami.5b08862>
- Gupta K, Bhattacharya S, Chattopadhyay D et al (2011) Ceria associated manganese oxide nanoparticles: synthesis, characterization and arsenic(V) sorption behavior. *Chem Eng J* 172:219–229. <https://doi.org/10.1016/j.cej.2011.05.092>
- Hokkanen S, Repo E, Lou S, Sillanpää M (2015) Removal of arsenic(V) by magnetic nanoparticle activated microfibrillated cellulose. *Chem Eng J* 260:886–894. <https://doi.org/10.1016/j.cej.2014.08.093>
- Hu JS, Zhong LS, Song WG, Wan LJ (2008) Synthesis of hierarchically structured metal oxides and their application in heavy metal ion removal. *Adv Mater* 20:2977–2982. <https://doi.org/10.1002/adma.200800623>
- Hua M, Zhang S, Pan B et al (2012) Heavy metal removal from water/wastewater by nanosized metal oxides: a review. *J Hazard Mater* 211–212:317–331. <https://doi.org/10.1016/j.jhazmat.2011.10.016>

- Huang X, Pan M (2016) The highly efficient adsorption of Pb(II) on graphene oxides: a process combined by batch experiments and modeling techniques. *J Mol Liq* 215:410–416. <https://doi.org/10.1016/j.molliq.2015.12.061>
- Ismail AA, El-Midany AA, Ibrahim IA, Matsunaga H (2008) Heavy metal removal using SiO₂-TiO₂ binary oxide: experimental design approach. *Adsorption* 14:21–29. <https://doi.org/10.1007/s10450-007-9042-4>
- Järup L, Berglund M, Elinder C et al (1998) Health effects of cadmium exposure: a review of the literature and a risk estimate. *Scand J Work Environ Health* 24:1–51
- Jena S (2012) Synthesis of ceria nanopowder for the removal of hexavalent chromium from synthetic Cr(VI) solution. Doctoral dissertation
- Jiangtao Z (2016) Ceria hollow nanospheres synthesized by hydrothermal method and their adsorption capacity. *Chin J Mater Res*. <https://doi.org/10.11901/1005.3093.2015.440>
- Kang D, Yu X, Ge M (2017) Morphology-dependent properties and adsorption performance of CeO₂ for fluoride removal. *Chem Eng J* 330:36–43. <https://doi.org/10.1016/j.cej.2017.07.140>
- Kasgoz H, Durmus A, Kasgoz A (2008) Enhanced swelling and adsorption properties of AAm-AMPSNa/clay hydrogel nanocomposites for heavy metal ion removal. *Polym Adv Technol* 19:213–220. <https://doi.org/10.1002/pat>
- Khan NA, Hasan Z, Jung SH (2013) Adsorptive removal of hazardous materials using metal-organic frameworks (MOFs): A review. *J Hazard Mater* 244–245:444–456. <https://doi.org/10.1016/j.jhazmat.2012.11.011>
- Kumar KY, Muralidhara HB, Nayaka YA et al (2013) Low-cost synthesis of metal oxide nanoparticles and their application in adsorption of commercial dye and heavy metal ion in aqueous solution. *Powder Technol* 246:125–136. <https://doi.org/10.1016/j.powtec.2013.05.017>
- Kuncham K, Nair S, Durani S, Bose R (2017) Efficient removal of uranium(VI) from aqueous medium using ceria nanocrystals: an adsorption behavioural study. *J Radioanal Nucl Chem* 313:101–112. <https://doi.org/10.1007/s10967-017-5279-x>
- Lee YC, Yang JW (2012) Self-assembled flower-like TiO₂ on exfoliated graphite oxide for heavy metal removal. *J Ind Eng Chem* 18:1178–1185. <https://doi.org/10.1016/j.jiec.2012.01.005>
- Li R, Li Q, Gao S, Shang JK (2012) Exceptional arsenic adsorption performance of hydrous cerium oxide nanoparticles: part A. Adsorption capacity and mechanism. *Chem Eng J* 185–186:127–135. <https://doi.org/10.1016/j.cej.2012.01.061>
- Li Z, Shen Y, Li X et al (2016) Synergistic catalytic removal of HgO and NO over CeO₂(ZrO₂)/TiO₂. *Catal Commun* 82:55–60. <https://doi.org/10.1016/j.catcom.2016.04.019> Short communication
- Lin KS, Chowdhury S (2010) Synthesis, characterization, and application of 1-D cerium oxide nanomaterials: a review. *Int J Mol Sci* 11:3226–3251. <https://doi.org/10.3390/ijms11093226>
- Lin J, Wu Y, Khayambashi A et al (2017) Preparation of a novel CeO₂/SiO₂ adsorbent and its adsorption behavior for fluoride ion. *Adsorpt Sci Technol*. <https://doi.org/10.1177/0263617417721588>
- Liu J, Zhao Z, Jiang G (2008) Coating Fe₃O₄ magnetic nanoparticles with humic acid for high efficient removal of heavy metals in water. *Environ Sci Technol* 42:6949–6954. <https://doi.org/10.1021/es800924c>
- Liu J, Cao J, Hu Y et al (2017) Adsorption of phosphate ions from aqueous by CeO₂ functionalized Fe₃O₄@SiO₂ core-shell magnetic nanomaterial. *Water Sci Technol* 76:2867–2875. <https://doi.org/10.2166/wst.2017.412>
- Mahapatra A, Mishra BG, Hota G (2013) Electrospun Fe₂O₃-Al₂O₃ nanocomposite fibers as efficient adsorbent for removal of heavy metal ions from aqueous solution. *J Hazard Mater* 258–259:116–123. <https://doi.org/10.1016/j.jhazmat.2013.04.045>
- Martin S, Griswold W (2009) Human health effects of heavy metals. *Environ Sci Technol Br Citiz* 15:1–6
- Mercado-Borrayo BM, Contreras R, Sánchez A et al (2018) Optimisation of the removal conditions for heavy metals from water: a comparison between steel furnace slag and CeO₂ nanoparticles. *Arab J Chem*. <https://doi.org/10.1016/j.arabjc.2018.01.008>
- Minovic-Arsic T, Kalijadis A, Matovic B et al (2016) Arsenic(III) adsorption from aqueous solutions on novel carbon cryogel/ceria nanocomposite. *Process Appl Ceram* 10:17–23. <https://doi.org/10.2298/PAC1601017M>
- Mohapatra M, Padhi T, Anand S, Mishra BK (2012) CTAB mediated Mg-doped nano Fe₂O₃: synthesis, characterization, and fluoride adsorption behavior. *Desalin Water Treat* 50:376–386. <https://doi.org/10.1080/19443994.2012.720411>
- Naim MM, Moneer AA, El-said GF (2012) Defluoridation of commercial and analar sodium fluoride solutions without using additives by batch electrocoagulation-flotation technique. *Desalin Water Treat* 44:110–117
- Nath BK, Chaliha C, Kalita E, Kalita MC (2016) Synthesis and characterization of ZnO:CeO₂:nanocellulose:PANI bionanocomposite. A bimodal agent for arsenic adsorption and antibacterial action. *Carbohydr Polym* 148:397–405. <https://doi.org/10.1016/j.carbpol.2016.03.091>
- Pan C, Zhang D, Shi L (2008a) CTAB assisted hydrothermal synthesis, controlled conversion and CO oxidation properties of CeO₂ nanoplates, nanotubes, and nanorods. *J Solid State Chem* 181:1298–1306. <https://doi.org/10.1016/j.jssc.2008.02.011>
- Pan C, Zhang D, Shi L, Fang J (2008b) Template-free synthesis, controlled conversion, and CO oxidation properties of CeO₂ nanorods, nanotubes, nanowires, and nanocubes. *Eur J Inorg Chem*. <https://doi.org/10.1002/ejic.200800047>
- Peng X, Luan Z, Ding J et al (2005) Ceria nanoparticles supported on carbon nanotubes for the removal of arsenate from water. *Mater Lett* 59:399–403. <https://doi.org/10.1016/j.matlet.2004.05.090>
- Priyadharsan A, Vasanthakumar V, Karthikeyan S et al (2017) Multifunctional properties of ternary CeO₂/SnO₂/rGO nanocomposites: visible light driven photocatalyst and heavy metal removal. *J Photochem Photobiol A Chem* 346:32–45. <https://doi.org/10.1016/j.jphotochem.2017.05.030>
- Qizheng CUI, Xiangting D, Jinxian W, Mei LI (2008) Direct fabrication of cerium oxide hollow nanofibers by electrospinning. *J Rare Earths* 26:664–669. [https://doi.org/10.1016/S1002-0721\(08\)60158-1](https://doi.org/10.1016/S1002-0721(08)60158-1)
- Raichur AM, Panvekar V (2002) Removal of As(V) by adsorption onto mixed rare earth oxides. *Sep Sci Technol* 37:1095–1108. <https://doi.org/10.1081/SS-120002243>
- Recillas S, Colón J, Casals E et al (2010) Chromium VI adsorption on cerium oxide nanoparticles and morphology changes during the process. *J Hazard Mater* 184:425–431. <https://doi.org/10.1016/j.jhazmat.2010.08.052>
- Sakthivel TS, Das S, Pratt CJ, Seal S (2017) One-pot synthesis of a ceria-graphene oxide composite for the efficient removal of arsenic species. *Nanoscale* 9:3367–3374. <https://doi.org/10.1039/C6NR07608D>
- Sharma R, Singh N, Gupta A et al (2014) Electrospun chitosan-polyvinyl alcohol composite nanofibers loaded with cerium for efficient removal of arsenic from contaminated water. *J Mater Chem A* 2:16669–16677. <https://doi.org/10.1039/C4TA02363C>
- Sun C, Li H, Zhang H et al (2005) Controlled synthesis of CeO₂ nanorods by a solvothermal method. *Nanotechnology* 16:1454–1463. <https://doi.org/10.1088/0957-4484/16/9/006>
- Sun W, Li Q, Gao S, Shang JK (2012) Exceptional arsenic adsorption performance of hydrous cerium oxide nanoparticles: part B. Integration with silica monoliths and dynamic treatment. *Chem Eng J* 185–186:136–143. <https://doi.org/10.1016/j.cej.2012.01.060>

- Talebzadeh F, Zandipak R, Sobhanardakani S (2016) CeO₂ nanoparticles supported on CuFe₂O₄ nanofibers as novel adsorbent for removal of Pb(II), Ni(II), and V(V) ions from petrochemical wastewater. *Desalin Water Treat* 57:28363–28377. <https://doi.org/10.1080/19443994.2016.1188733>
- Taylor EW (1959) International standards for drinking-water. *Nature* 183:867–868. <https://doi.org/10.1038/183867b0>
- Vaizoğullar AI, Balci A, Kula İ, Ugurlu M (2016) Preparation, characterization, and adsorption studies of core@shell SiO₂@CeO₂ nanoparticles: a new candidate to remove Hg(II) from aqueous solutions. *Turk J Chem* 40:565–575. <https://doi.org/10.3906/kim-1507-7>
- Vantomme A, Yuan ZY, Du G, Su BL (2005) Surfactant-assisted large-scale preparation of crystalline CeO₂ nanorods. *Langmuir* 21:1132–1135. <https://doi.org/10.1021/la047751p>
- Xiao H, Ai Z, Zhang L (2009) Nonaqueous sol–gel synthesized hierarchical CeO₂ nanocrystal microspheres as novel adsorbents for wastewater treatment. *J Phys Chem C* 113:16625–16630. <https://doi.org/10.1021/jp9050269>
- Xu W, Wang J, Wang L et al (2013) Enhanced arsenic removal from water by hierarchically porous CeO₂–ZrO₂ nanospheres: role of surface- and structure-dependent properties. *J Hazard Mater* 260:498–507. <https://doi.org/10.1016/j.jhazmat.2013.06.010>
- Yamamura S, Bartram J, Csanady M et al (2003) Drinking water guidelines and standards. Arsenic, water, and health: the state of the art. World Health Organization, Geneva, Switzerland
- Yari S, Abbasizadeh S, Mousavi SE et al (2015) Adsorption of Pb(II) and Cu(II) ions from aqueous solution by an electrospun CeO₂ nanofiber adsorbent functionalized with mercapto groups. *Process Saf Environ Prot* 94:159–171. <https://doi.org/10.1016/j.psep.2015.01.011>
- Zhang D, Yan T, Pan C et al (2009) Carbon nanotube-assisted synthesis and high catalytic activity of CeO₂ hollow nanobeads. *Mater Chem Phys* 113:527–530. <https://doi.org/10.1016/j.matchemphys.2008.09.052>
- Zhang T, Li Q, Liu Y et al (2011) Equilibrium and kinetics studies of fluoride ions adsorption on CeO₂/Al₂O₃ composites pretreated with non-thermal plasma. *Chem Eng J* 168:665–671. <https://doi.org/10.1016/j.cej.2011.01.054>
- Zhang T, Li Q, Mei Z et al (2013) Adsorption of fluoride ions onto non-thermal plasma-modified CeO₂/Al₂O₃ composites. *Desalin Water Treat* 52:3367–3376. <https://doi.org/10.1080/19443994.2013.800324>
- Zhao G, Li J, Ren X et al (2011) Few-layered graphene oxide nanosheets for heavy metal ion pollution management. *Environ Sci Technol* 45:10454–10462. <https://doi.org/10.1021/es203439v>
- Zhong LS, Hu JS, Cao AM et al (2007) 3D flowerlike ceria micro/nanocomposite structure and its application for water treatment and CO removal. *Chem Mater* 19:1648–1655. <https://doi.org/10.1021/cm062471b>